Electrostatic potential and double layer force in a semiconductor-electrolyte-semiconductor heterojunction

S. J. Miklavcic and E. Said
Department of Science and Technology, Linköping University, Campus Norrköping, S-601 74, Norrköping, Sweden
(Received 23 August 2006; published 28 December 2006)

This paper reports a theoretical study of the electrostatic potential within a so-called *pen*-heterojunction made up of two semi-infinite, doped semiconductor media separated by an electrolyte region. An external potential is then applied across the entire system. Both the electrostatic potentials and double layer surface forces are studied as functions of the usual double layer system properties, semiconductor properties such as doping concentrations of acceptor and donator atoms, as well as applied potential. We find that both attractive and repulsive forces are possible depending on the surface charges on the electrolyte-semiconductor interfaces, and that these forces can be significantly modified by the applied potential and by the doping levels in the semiconductors.

DOI: 10.1103/PhysRevE.74.061606 PACS number(s): 68.15.+e, 68.35.Md, 68.47.Fg

I. INTRODUCTION

The electrical double layer adjacent to charged macroscopic surfaces has been an active subject of research for a long time. Since the founding work of Gouy and Chapman, Verwey, and Overbeek [1] on symmetric electrolytes adjacent to constant potential surfaces, we have seen extensions to asymmetric electrolytes [2], constant charge and charge regulating surfaces [3,4], nonuniformly charged surfaces [5–8], and surfaces of nonuniform shape, i.e., rough surfaces [9–14]. In addition, steps have been taken to account for higher-order statistical mechanical effects, such as ion-ion electrostatic correlations and excluded volume effects [15–17]. These extensions cover a range of features that appear in real systems and thus represent the true nature of inhomogeneous electrolyte systems.

In this paper we study a new incidence of the electrical double layer, possibly exemplifying a new area of application of double layer theory to contemporary electronics technology. In recent years, with the growing interest in developing novel, environmentally friendly, cheap, and effective electronics devices, some effort has gone into understanding the workings of organic and aqueous electronics systems [18–22]. In such systems it is no longer just the electronic components (free electrons and holes) that are important to system function, but also the interaction between the ionic components (the electrolyte ions). Although the main focus of attention has been on dynamic behavior and properties, the steady-state properties too are significant.

Two instruments are now in common use to monitor the double layer interaction between two charged macroscopic surfaces in an electrolyte: the surface force apparatus (SFA) [23,24] and the atomic force microscope (AFM) [25]. The SFA was recently featured in studies of systems (usually involving molecular smooth and uniformly thick mica sheets with approximately 1 cm^2 of exposed area) that allow one to externally control electrical conditions in order to manipulate the surface force. As one example, Connor, Horn, and Antelmi [26,27] have replaced one of the two mica surfaces with a mercury interface. They then externally applied an electrical potential to the fluid mercury surface and monitored the changes to the electrical double layer as well as changes in the shape of the mercury-water interface. Fréchette and Vanderlick [28–30], on the other hand, modified the SFA by replacing one mica surface with a gold surface and applied an external potential difference across the triple layer (mica-electrolyte-gold) system: in effect, converting the SFA into an electrochemical device. Analogous developments have also been made using the AFM in the colloid probe arrangement [31,32]. These developmental efforts can potentially extend the range of application of the SFA and AFM to give greater insight into the workings of electronic devices incorporating aqueous electrolytes and/or polymer electrolytes.

The next step motivated by the two SFA studies is to consider the possibility of the outer two materials being doped (p and n) semiconductors possessing intrinsic free charges as well as being predoped to specified degrees. The media therefore bear within them fixed doped charges as well as free electron and hole carriers. Placed in parallel with an intervening electrolyte (e) in chemical equilibrium with a bulk phase, they form what can be called a *pen*-heterojunction in analogy with accepted semiconductor terminology; the electrolyte (e) replaces the undoped intrinsic (i) semiconductor material that is normally found in a so-called *pin*-heterojunction. Although such a *pen* system with an applied potential has not, to our knowledge, been studied using the SFA or AFM force measuring devices, it can be useful to precede such work with a theoretical investigation of the system's double layer properties—both the electrostatic potential and the double layer interaction. Apart from providing general insight, the theoretical results can possibly lead to suggestions of materials or conditions for best experimental study. Here, we focus primarily on the electrostatic properties of the triple layer system, as a function of intervening electrolyte thickness, applied external potential, surface charge, bulk concentration of the intervening electrolyte, as well as doping and intrinsic charge concentration in the semiconductors. Since this already introduces a large number of variables to study we leave out any electrochemical effects of the applied potential on the adsorption of aqueous species such as reported in the SFA work of Fréchette and

 ©2006 The American Physical Society

Vanderlick [29,30] and the AFM work of Wang *et al.* and Barten *et al.* [31,32].

The analysis and study is restricted to the steady state. A full study requires expressions for the charge distributions inside the semiconductor materia, which we assume are sufficiently thick so as to be treated as infinite. In Sec. II we provide a phenomenological derivation of expressions for these distributions since a sufficiently useful thermodynamic description of these charge distributions does not appear to be explicitly available in the semiconductor literature. With these, the mean-field electrostatic potential profile across the triple layer region is then considered in Sec. III; both exact and some simple, yet reasonable approximations are given. In Sec. IV numerical results for symmetric univalent electrolytes are provided and discussed. We end the paper with a short summary and indicate directions along which this work can develop.

II. THERMODYNAMIC CHARGE DISTRIBUTION IN SEMI-INFINITE SEMICONDUCTORS

Consider first the case of two semi-infinite, semiconductor half-spaces in mathematical contact at $z=0$. The media are continuous semiconductors each doped differently to different extents. The medium defined for $z<0$ is doped with acceptor type atoms to a uniform concentration of N_a, while the medium $z>0$ is uniformly doped with donor type atoms to a concentration N_d. The semiconductors are thus p type for $z<0$ and n type for $z>0$ with an excess of free holes and electrons, respectively. The heterojunction they form is then a pn junction. In each of the media the charge bearers are electrons, holes, and impurity atoms. The first two types are mobile charge carriers while the doping atoms introduce a neutralizing fixed background of uniform charge. At equilibrium the local steady state concentrations of the mobile charge carriers are denoted $n(z)$ for electrons (negative) and $p(z)$ for holes (positive). Clearly, these functions will exhibit discontinuities at the junction $z=0$.

At equilibrium and in the absence of an externally applied potential, a potential difference V_{BI} is set up across the outer extremes of the p-type- and n-type-doped semiconductors when their ends are in contact (or, as will be the case later, in close proximity separated by an electrolyte). The discontinuities in the conduction and valence bands of these materials give rise to charge carrier accumulation/depletion regions at the interfaces, which is manifested in the built-in potential V_{BI} in order to maintain chemical equilibrium. The value of V_{BI} is a function of the chemical composition of the materials and of the doping levels; it can be determined by the constraint that the chemical potentials of the electrons (the Fermi levels) be the same in both semiconductors. Note that the accumulation/depletion effects at the respective semiconductor interfaces can also, or alternatively, be represented as surface charge(s) σ at the junction(s).

At infinite distance from the junction, an external bias potential V_{app} is applied over and above the built-in potential V_{BI}. The net effect is governed by the difference $V_D=V_{BI}-V_{\text{app}}$, which for our purposes is the only quantity that we need to specify. For simplicity, we can assume grounding at $z=-\infty$ and a net potential difference of V_D at $z=+\infty$. At steady state, a continuous electric potential profile, $\psi(z)$, will be set up through the system satisfying the far field conditions

$$\psi \to \begin{cases} 0, & z \to -\infty, \\ V_D, & z \to +\infty. \end{cases} \quad (1)$$

These limits naturally imply the weaker condition

$$\frac{\partial \psi}{\partial z} \to 0, \quad z \to \pm\infty, \quad (2)$$

on the electric field. In turn this is consistent with the physical condition of overall system electroneutrality. Alternately, electroneutrality can be expressed as the integral

$$\int_{-\infty}^{\infty} \rho(z) dz = 0,$$

where

$$\rho(z) = q[p(z) - n(z) + N_d H(z) - N_a H(-z)] \quad (3)$$

is the local charge density. $H(z)$ is the Heaviside step function. Necessary conditions for electroneutrality are the limits $\rho(z) \to 0$, as $z \to \pm\infty$, or

$$p(z \to -\infty) - n(z \to -\infty) - N_a = 0,$$

$$p(z \to \infty) - n(z \to \infty) + N_d = 0. \quad (4)$$

We shall make use of notations customary in the semiconductor field $p(z\to-\infty)=p_p$, $n(z\to-\infty)=n_p$, $p(z\to\infty)=p_n$, and $n(z\to\infty)=n_n$. In each semiconductor the continually ongoing electron-hole pair productions and annihilations result at finite temperature in the steady state relations [33]

$$(n_{i,p})^2 = n_p p_p,$$

$$(n_{i,n})^2 = n_n p_n, \quad (5)$$

where $n_{i,n}$ and $n_{i,p}$ are the temperature-dependent, intrinsic concentrations specific for the given semiconductors. Moreover, in the steady state the individual charge carriers are in chemical potential equilibrium and thus there exist, in a mean-field description, simple relations between the concentrations of the mobile species at the two extremes $\pm\infty$

$$\frac{n_n}{n_p} = \frac{p_p}{p_n} = e^{q\beta V_D}, \quad (6)$$

where $\beta=1/k_B T$, k_B is Boltzmann's constant and T is the temperature.

Equations (4)–(6) allow for the equilibrium electron and hole concentrations infinitely far from the junction to be determined in terms of the semiconductor intrinsic concentrations, doping concentrations, and the net potential difference V_D. In fact, Eqs. (4) and (5) are equivalent to a set of quadratic equations from which one immediately has (for $N_a, N_d \neq 0$)

$$n_n = \frac{N_d}{2} + \frac{N_d}{2}\sqrt{1 + \frac{4(n_{i,n})^2}{N_d^2}} \approx N_d + \frac{(n_{i,n})^2}{N_d}, \quad \text{for } n_{i,n} \ll N_d,$$

$$p_p = \frac{N_a}{2} + \frac{N_a}{2}\sqrt{1 + \frac{4(n_{i,p})^2}{N_a^2}} \approx N_a + \frac{(n_{i,p})^2}{N_a}, \quad \text{for } n_{i,p} \ll N_a. \tag{7}$$

Provided there exist no further discontinuities in the semi-infinite media, a continuous and piecewise smooth transition from one spatial extreme $(-\infty)$ to the other (∞), can be effected using a local Boltzmann distribution weighted by the locally varying electrostatic potential ψ. The statistical mechanics of electrons and holes are actually described by Fermi-Dirac distribution functions. However, provided the electron (or hole) energy (minus the chemical potential) is sufficiently large compared to k_BT, the distribution functions will approximately be of the Boltzmann type [36]. The local charge density in the semiconductor regions, consistent with the argument described by Eqs. (1) and (4)–(6) is then

$$\rho(z) = q\begin{cases} p_p e^{-q\beta\psi(z)} - n_n e^{-q\beta V_D} e^{q\beta\psi(z)} - N_a, & z < 0, \\ p_p e^{-q\beta\psi(z)} - n_n e^{-q\beta V_D} e^{q\beta\psi(z)} + N_d, & z > 0. \end{cases}$$

Applying (4) once again results in an even more useful expression for the density,

$$\rho(z) = q\begin{cases} p_p(e^{-q\beta\psi(z)} - 1) \\ \quad - n_n e^{-q\beta V_D}(e^{q\beta\psi(z)} - 1), & z < 0, \\ p_p e^{-q\beta V_D}(e^{-q\beta(\psi(z)-V_D)} - 1) \\ \quad - n_n(e^{q\beta(\psi(z)-V_D)} - 1), & z > 0, \end{cases} \tag{8}$$

where again the constant coefficients n_n and p_p are given by Eq. (7). Equation (8) describes the equilibrium charge density. The foregoing derivation is based on equilibrium arguments and differs from the usual derivation based on large-time limits of solutions of diffusion equations [34–36].

When the two semi-infinite, semiconductors are separated by a third, undoped semiconductor medium of intrinsic charge bearer concentration n_i and thickness d the system forms a *pin* junction of a transistor. Alternately, we shall be focusing on a modified version of this where the intervening medium is a univalent electrolyte solution of ion density n_e, molar concentration c_e, and thickness d. Consequently, this triple-layer system could be analogously called a *pen* junction (see Fig. 1). The above expression for the steady-state or equilibrium density distribution (8) can then be used in the doped semiconductor regions if modified slightly to account for the shift in spatial coordinate definition. The complete specification of charge density for the *pen*-heterojunction is then

$$\rho(z) = q\begin{cases} p_p(e^{-q\beta\psi(z)} - 1) \\ \quad - n_n e^{-q\beta V_D}(e^{q\beta\psi(z)} - 1), & z < 0, \\ n_e e^{-q\beta\psi(z)} - n_e e^{q\beta\psi(z)}, & 0 < z < d, \\ p_p e^{-q\beta V_D}(e^{-q\beta(\psi(z)-V_D)} - 1) \\ \quad - n_n(e^{q\beta(\psi(z)-V_D)} - 1), & z > d. \end{cases} \tag{9}$$

In Eq. (9) the assumption of a univalent electrolyte as intervening medium is explicitly taken and we adopt the usual mean-field Boltzmann approach even in this region. This self-consistent expression for the equilibrium distribution of charges throughout a heterogeneous *pen*-junction is a key result of the paper. A cursory examination of the standard texts in this subject [34–36] has not revealed a similar discussion.

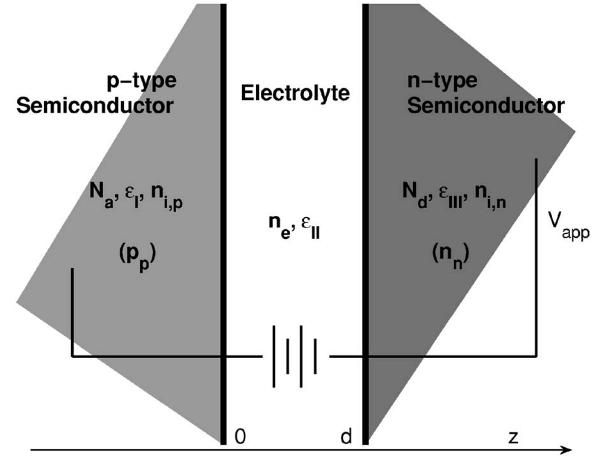

FIG. 1. Schematic of the *pen*-heterojunction.

Although the experimental variables N_a, $n_{i,p}$, N_d, $n_{i,n}$ actually characterize the properties of the semiconductors, only the parameters p_p and n_n come into play in the numerics. Consequently, we shall only specify numerical values of p_p and n_n in our calculations since we do not model any particular materia in this paper.

III. ELECTROSTATIC POTENTIAL PROFILE

With the piecewise defined charge density specified, the corresponding electrostatic potential profile in the system can be determined by application of standard electrostatic principles. In general, the three dielectric materia form a sandwich occupying the region $-L_1 \le z \le 0$, where L_1 can be infinite, the electrolyte region $0 \le z \le d$, and the interval $d \le z \le d + L_2$, where L_2 can be infinite. We denote the entire space Γ. The everywhere continuous and piecewise smooth electrostatic potential can be obtained locally as the solution of the Poisson equation

$$\frac{d}{dz}\left(\epsilon(z)\frac{d}{dz}\psi(z)\right) = -\frac{\rho(z)}{\epsilon_0}, \quad z \in \Gamma, \tag{10}$$

where $\epsilon(z)$ is a piecewise constant dielectric permittivity function defined as

$$\epsilon(z) = \begin{cases} \epsilon_{\mathrm{I}}, & z < 0, \\ \epsilon_{\mathrm{II}}, & 0 < z < d, \\ \epsilon_{\mathrm{III}}, & z > d \end{cases}$$

for the composite system. Apart from the requirements on ψ at the extremes of z, Eqs. (1) and (2), the electrostatic potential is also subject to the following matching conditions at the interfaces $z=0$ and $z=d$:

$$\psi(0^+) = \psi(0^-),$$

$$\psi(d^+) = \psi(d^-),$$

$$\epsilon_{\mathrm{II}}\frac{\partial\psi}{\partial z}(0^+) - \epsilon_{\mathrm{I}}\frac{\partial\psi}{\partial z}(0^-) = -\frac{\sigma_p}{\epsilon_0},$$

$$\epsilon_{\mathrm{III}}\frac{\partial\psi}{\partial z}(d^+) - \epsilon_{\mathrm{II}}\frac{\partial\psi}{\partial z}(d^-) = -\frac{\sigma_n}{\epsilon_0}. \tag{11}$$

The first of these equations imply the continuity of the electrostatic potential across the electrolyte-semiconductor interfaces. The last two equations impose the condition that the discontinuity of the electric displacement ($\vec{D}=\epsilon\vec{E}$) at an interface be equal to the intrinsic surface charge there. Note also that only by allowing for charge and potential distributions in all three regions is it possible to simultaneously impose constant charge conditions [Eqs. (11)] and constant potential conditions [Eqs. (1)]. Only one of either such condition can be applied in the case of a single medium, since the governing equation for the potential is of second order.

A. Linear density approximation

The problem of determining the potential distribution under arbitrary conditions will generally involve numerical techniques. However, under certain circumstances the problem can be simplified sufficiently to enable an approximate analytic solution. An analytic solution is in fact a useful guide to confirm the physical correctness of the model and even to provide a quantitative check on numerical solutions in restricted cases. In this and the next subsection, we provide such analytic solutions. The most obvious simplification is based on the assumption of low difference potentials V_D. In such cases the potential function will satisfy the condition $|\psi| \leq |V_D| < k_BT/q$. Consistent with this assumption, the volume charge density $\rho(z)$ in Eq. (9) will to a good approximation be given by

$$\rho(z) \approx \begin{cases} -\dfrac{q^2\beta}{\epsilon_{\mathrm{I}}\epsilon_0}[p_p + n_n(1-q\beta V_D)]\psi(z), & z<0, \\ -\dfrac{2q^2\beta n_e}{\epsilon_{\mathrm{II}}\epsilon_0}\psi(z), & 0<z<d, \\ -\dfrac{q^2\beta}{\epsilon_{\mathrm{III}}\epsilon_0}[p_p(1-q\beta V_D)+n_n] \\ \quad \times[\psi(z)-V_D], & z>d. \end{cases} \tag{12}$$

Consequently, the Poisson equation becomes a piecewise linear differential equation for the potential, ψ. A general solution of Eq. (10) with Eq. (12) that satisfies the electroneutrality conditions (1) and (2) is simply

$$\psi(z) = \begin{cases} e^{\kappa_p z}B_I, & z \leq 0, \\ e^{-\kappa z}A_{\mathrm{II}} + e^{\kappa z}B_{\mathrm{II}}, & 0 \leq z \leq d, \\ e^{-\kappa_n z}A_{\mathrm{III}} + V_D, & z \geq d. \end{cases} \tag{13}$$

Here, $\kappa_p^2 = q^2\beta[p_p + n_n(1-q\beta V_D)]/\epsilon_{\mathrm{I}}\epsilon_0$, $\kappa_n^2 = q^2\beta[n_n + p_p(1-q\beta V_D)]/\epsilon_{\mathrm{III}}\epsilon_0$, and $\kappa^2 = 2q^2\beta n_e/\epsilon_{\mathrm{II}}\epsilon_0$. The latter defines the usual Debye screening parameter of electrolyte theory [1]. The inequality $0 < V_D < k_BT/q$ ensures that κ_n^2 and κ_p^2 will always be positive. Hence, in their capacity as scaling factors in the exponential functions κ_n and κ_p are well defined, real-valued screening parameters governing the decay of the potential and field in the two respective doped semiconductors. The constants B_{I}, A_{II}, B_{II}, andA_{III} are determined upon application of the remaining boundary conditions (11). These give the following inhomogeneous system of four equations in the four constants:

$$B_{\mathrm{I}} = A_{\mathrm{II}} + B_{\mathrm{II}},$$

$$\epsilon_{\mathrm{I}}\kappa_p B_{\mathrm{I}} + \epsilon_{\mathrm{II}}\kappa(A_{\mathrm{II}} - B_{\mathrm{II}}) = -\sigma_p/\epsilon_0,$$

$$A_{\mathrm{III}}e^{-\kappa_n d} + V_D = A_{\mathrm{II}}e^{-\kappa d} + B_{\mathrm{II}}e^{\kappa d},$$

$$-\epsilon_{\mathrm{III}}\kappa_n A_{\mathrm{III}}e^{-\kappa_n d} + \epsilon_{\mathrm{II}}\kappa(A_{\mathrm{II}}e^{-\kappa d} - B_{\mathrm{II}}e^{\kappa d}) = -\sigma_n/\epsilon_0$$

which can be uniquely inverted. The first two lead to

$$B_{\mathrm{I}} = \frac{2\epsilon_{\mathrm{II}}\kappa B_{\mathrm{II}} - \sigma_p/\epsilon_0}{(\epsilon_{\mathrm{I}}\kappa_p + \epsilon_{\mathrm{II}}\kappa)},$$

$$A_{\mathrm{II}} = \frac{(\epsilon_{\mathrm{II}}\kappa - \epsilon_{\mathrm{I}}\kappa_p)B_{\mathrm{II}} - \sigma_p/\epsilon_0}{(\epsilon_{\mathrm{I}}\kappa_p + \epsilon_{\mathrm{II}}\kappa)},$$

while the last two equations result in the system $AX=Y$, where

$$A = \begin{pmatrix} -1 & [\epsilon_{\mathrm{II}}\kappa\cosh(\kappa d) + \epsilon_{\mathrm{I}}\kappa_p\sinh(\kappa d)] \\ \epsilon_{\mathrm{III}}\kappa_n & \epsilon_{\mathrm{II}}\kappa[\epsilon_{\mathrm{II}}\kappa\sinh(\kappa d) + \epsilon_{\mathrm{I}}\kappa_p\cosh(\kappa d)] \end{pmatrix}$$

and

$$X = \begin{pmatrix} A_{\mathrm{III}}e^{-\kappa_n d} \\ \dfrac{2B_{\mathrm{II}}}{(\epsilon_{\mathrm{I}}\kappa_p + \epsilon_{\mathrm{II}}\kappa)} \end{pmatrix}, \quad Y = \begin{pmatrix} V_D + \Xi_p \\ \sigma_n/\epsilon_0 - \Xi_p \end{pmatrix},$$

where $\Xi_p = \sigma_p e^{-\kappa d}/\epsilon_0(\epsilon_{\mathrm{I}}\kappa_p + \epsilon_{\mathrm{II}}\kappa)$. The system is to be solved for constants A_{III} and B_{II}. For reasons of space, we do not give this solution explicitly nor do we give any explicit numerical examples of this approximation. One justification for including this result here is that with the linear model one can study with minimal effort the qualitative behavior of the system and its dependence on the principal parameters. Although quantitatively limited in accuracy such a study of parameter space may be useful to the experimentalist.

B. Counterion dominant approximation

In the more general case of a non-negligible net difference potential $V_D = V_{BI} - V_{\mathrm{app}}$, it is reasonable that the potential in the semi-infinite half-space $z > d$ will be of the order of V_D, while in the half-space $z < 0$ the potential will be quite low in magnitude. In the central region, however, the potential can be significant. It is possible to exploit these expectations in order to once again simplify the problem. In quantitative terms, the potential in the two outer regions can be assumed to approach the respective limits sufficiently rapidly that, on the left, $\psi \lesssim k_BT/q$, while on the right, $|\psi - V_D| \lesssim k_BT/q$, even though V_D itself is not necessarily small. Any errors that arise as a result of these assumptions are most likely to

appear within the first Debye lengths κ_p and κ_n of these respective semi-infinite regions. Furthermore, in the central region the magnitude of the potential can be sufficiently large, $|\psi| \geq k_B T/q$ (especially if V_D is significant), that the counterion concentration will dominate over the co-ion concentration in the total volume charge density $\rho(z)$. By this we mean that $\exp(-q\beta\psi) \leq 1 \ll \exp(q\beta\psi)$. Consequently, the charge density would be approximately

$$\rho(z) \approx \begin{cases} -\dfrac{q^2}{k_B T}(p_p + n_n e^{-q\beta V_D})\psi(z), & z<0, \\ -q n_e e^{q\beta\psi(z)}, & 0<z<d, \\ -\dfrac{q^2}{k_B T}(p_p e^{-q\beta V_D} + n_n)(\psi(z)-V_D), & z>d. \end{cases} \tag{14}$$

As a consequence of the linear potential-density relation in the outer two regions, the potential is similar in appearance to Eq. (13):

$$\psi(z) = \begin{cases} e^{\kappa_p z} B_{\mathrm{I}}, & z \leq 0, \\ e^{-\kappa_n z} A_{\mathrm{III}} + V_D, & z \geq d. \end{cases} \tag{15}$$

For convenience we have used the same notation for the decay length parameters, although they are now defined to be $\kappa_p^2 = q^2\beta(p_p + n_n e^{-q\beta V_D})/\epsilon_{\mathrm{I}}\epsilon_0$, $\kappa_n^2 = q^2\beta(n_n + p_p e^{-q\beta V_D})/\epsilon_{\mathrm{III}}\epsilon_0$. The two constants B_{I} and A_{III} in Eq. (15) are specified in terms of the solution within the electrolyte medium through the boundary conditions (11). Specifically,

$$q\beta B_{\mathrm{I}} = q\beta\psi(0^+),$$

$$q\beta A_{\mathrm{III}} = q\beta e^{\kappa_n d}[\psi(d^-) - V_D]. \tag{16}$$

As argued, the Poisson-Boltzmann equation (10) plus Eq. (9) describing the potential ψ in $0<z<d$ is approximately

$$\frac{d^2}{dz^2}\psi = \frac{q}{\epsilon_{\mathrm{II}}\epsilon_0} n_e \exp(q\beta\psi), \quad z \in (0,d)$$

or, in terms of nondimensional variables $s = \kappa z$, $y = q\psi/k_B T$,

$$\frac{d^2 y}{ds^2} = \frac{1}{2}\exp(y), \quad s \in (0,\kappa d). \tag{17}$$

A first integral of Eq. (17) can be effected in the standard manner to give

$$\left(\frac{dy}{ds}\right)^2\bigg|_y - \left(\frac{dy}{ds}\right)^2\bigg|_{y_0} = \exp(y) - \exp(y_0) \tag{18}$$

for $s \in (0,\kappa d)$, $y_0 = y(s_0)$, where s_0 is some convenient reference point of the coordinate variable.

A second integral of Eq. (17) will be possible with the following mathematical construct. Although a physical solution to Eq. (17) is defined only in the closed interval $[0,\kappa d]$, we consider for the present the extension of the solution beyond this interval. We choose s_0 to be that first point in $(-\infty,\infty)$ beyond $[0,d]$ at which the derivative of the extended function vanishes. That is, we choose s_0 to be an extreme point—in fact a minimum point—of the extended potential. Thus, we suppose

$$\xi := \exp[y(s_0)],$$

$$y'(s_0) := 0. \tag{19}$$

Since s_0 is a minimum point, the potential y in $[0,\kappa d]$ will be an increasing function of s. Consequently, the order of the terms in Eq. (18) can be maintained when a square root is taken. This gives

$$\frac{dy}{ds} = \pm\sqrt{\exp(y) - \xi}, \tag{20}$$

where the sign $(+ve)$ must be chosen to agree with the expected sign of the derivative. By defining a new dependent variable $\phi = \exp(-y/2)$, Eq. (20) can be rearranged and rewritten in integral form as

$$\int^{\phi} \frac{d\theta}{\sqrt{1-\xi\theta^2}} = -\frac{1}{2}s + C,$$

where C is a generic integration constant. The above integral has an explicit function representation

$$\int^{\phi} \frac{d\theta}{\sqrt{1-\xi\theta^2}} = \frac{1}{\sqrt{\xi}}\arcsin(\sqrt{\xi}\phi) \Rightarrow \arcsin(\xi^{\frac{1}{2}}\phi) = -\frac{1}{2}\xi^{1/2}s + C \Rightarrow \phi(s) = \xi^{-1/2}\sin\left(C - \frac{1}{2}\xi^{1/2}s\right).$$

Using either of the conditions in Eq. (19) we find that the constant C must satisfy

$$C = \frac{1}{2}\xi^{1/2}s_0 + (2n-1)\frac{\pi}{2}, \quad n = 1,2,3,\ldots .$$

Although an academic point (as an analysis will show), the root $n=1$ is the only physically relevant one to ensure the correct monotonicity in the potential. Consequently, the function

$$\phi(s) = \xi^{-1/2}\cos\left(\frac{1}{2}\xi^{1/2}(s_0 - s)\right) \tag{21}$$

clearly satisfies Eq. (20) and condition (19). From Eq. (21) we see that for a physically relevant solution we must have that $s \in (s_0 - \pi\xi^{-1/2}, s_0 + \pi\xi^{-1/2})$.

Still remaining to be determined are the unknown parameters ξ and s_0. These, together with the constants, B_{I} and A_{III}, are determined by applying the boundary conditions (11) which, after some rewriting, reduce to the following inhomogeneous algebraic system:

$$-2\epsilon_{\mathrm{I}}\kappa_p \ln[\phi(0)] + 2\epsilon_{\mathrm{II}}\kappa \left.\frac{d\phi}{ds}\right|_0 \frac{1}{\phi(0)} = -\frac{q\beta\sigma_p}{\epsilon_0},$$

$$2\epsilon_{\mathrm{III}}\kappa_n \ln[\phi(\kappa d)] + 2\epsilon_{\mathrm{II}}\kappa \left.\frac{d\phi}{ds}\right|_{\kappa d} \frac{1}{\phi(\kappa d)} = -\epsilon_{\mathrm{III}}\kappa_n q\beta V_D - \frac{q\beta\sigma_n}{\epsilon_0}. \tag{22}$$

In turn, using Eq. (21), these become

$$-2\epsilon_{\rm I}\kappa_p \ln\left[\xi^{-1/2}\cos\left(\frac{\xi^{1/2}s_0}{2}\right)\right] + \epsilon_{\rm II}\kappa\xi^{1/2}\tan\left(\frac{\xi^{1/2}s_0}{2}\right) = -\frac{q\beta\sigma_p}{\epsilon_0},$$

$$2\epsilon_{\rm III}\kappa_n \ln\left[\xi^{-1/2}\cos\left(\frac{\xi^{1/2}}{2}(s_0-\kappa d)\right)\right] + \epsilon_{\rm II}\kappa\xi^{1/2}\tan\left(\frac{\xi^{1/2}}{2}(s_0-\kappa d)\right),$$

$$= -\epsilon_{\rm III}\kappa_n q\beta V_D - \frac{q\beta\sigma_n}{\epsilon_0}. \tag{23}$$

We therefore arrive at two transcendental equations in the two unknowns, $\xi^{1/2}$and s_0. Equation (23) is a nonlinear system, which can only be solved in general by numerical means. However, once done the solution pair can be inserted in Eq. (16) to produce a potential profile everywhere throughout the junction. Once again, for reasons of space we do not provide any explicit numerical examples, but place numerical focus instead on the symmetric electrolyte case described in the next section. The results of the present approximation, however, involve little more than the familiar trigonometric functions and are therefore easier to implement than the elliptic functions that arise in the symmetric electrolyte model given below. The above results might therefore be of more immediate use to the experimentalist for a first analysis of measurements.

C. Symmetric electrolyte

The full double layer problem with difference potential can be solved in a manner similar to the counterion-only approximation. The Poisson-Boltzmann equation in $z \in (0,d)$, including both co-ion and counterion distributions becomes

$$\frac{d^2\psi}{dz^2} = \frac{qn_e}{\epsilon_{\rm II}\epsilon_0}[\exp(q\beta\psi) - \exp(-q\beta\psi)].$$

To solve this we follow the method of Refs. [2,37,41]. In similar spirit to the previous section, we consider the extension of the function ψ to a new function whose domain of definition extends beyond $(0,d)$. The restriction of this new function (which satisfies the conditions at $z=0$ and $z=d$) to the given interval will be the solution we seek. For convenience we again use ψ to denote both these two functions. Now introduce the new dependent variable $y=q\beta[\psi(z)-\psi(z_0)]$. That is, the difference between the normalized potential at an arbitrary position, z, and the normalized potential value at the extremum point $z=z_0$, where $d\psi/dz=0$. In nondimensional form the Poisson-Boltzmann equation becomes

$$\frac{d^2y}{ds^2} = \frac{1}{2}[\exp(y)\xi^{-1} - \exp(-y)\xi],$$

where again we employ the variable $s=\kappa z$ [with $s \in (0,\kappa d)$ referring to the physically relevant interval] and define $\xi := \exp[-q\beta\psi(z_0)]$. For the sake of argument we assume in this discussion that $\psi \geq 0$ in which case $0<\xi<1$ (although, in the numerical implementation, both positive and negative potentials are accommodated). A first integral again can be effected giving

$$\left(\frac{dy}{ds}\right)^2\bigg|_y = [\exp(y)\xi^{-1} + \exp(-y)\xi + C], \tag{24}$$

where C is determined by the zero derivative condition at the maximum $s=s_0$, where $y=0$ and $y'=0$:

$$C = -(\xi + \xi^{-1}).$$

Introducing the variable $\phi=\exp(y)>\xi>0$ (in fact $\phi>1$), the first integral can be written as

$$\frac{d\phi}{ds} = +\frac{1}{\xi^{1/2}}\sqrt{\xi^2\phi - (\xi^2+1)\phi^2 + \phi^3}$$
$$= +\xi^{1/2}\sqrt{\phi(\phi-1)(\phi\xi^{-2}-1)}, \tag{25}$$

where the positive root has been taken to ensure a monotonically increasing potential. The order of the terms within the factors under the root sign is important to ensure their positivity. A primitive to Eq. (25) can be provided, at least formally. Define $\phi^{-1}=t^2$ we have

$$\int_{1/\sqrt{\phi}}^{1} \frac{dt}{\sqrt{(1-\xi t^2)(1-t^2)}} = \frac{1}{2\xi^{1/2}}(s-s_0) =: u, \tag{26}$$

where the limits on the integral satisfy the condition at the minimum and thereby conform to the expected magnitude of ϕ. The left-hand side of Eq. (26) is an elliptic integral satisfied by the Jacobi elliptic function $\mathrm{cd}(u,\xi)$, with argument u and modulus ξ [38–40]. Thus, the physically relevant potential for $s \in (0,\kappa d)$ is obtained from the relation

$$\frac{1}{\phi(s)} = \mathrm{cd}^2\left(\frac{(s-s_0)}{2\xi^{1/2}},\xi\right) = \exp(-y). \tag{27}$$

As in the preceding section the hitherto unknowns, s_0 and ξ, are determined by application of the boundary conditions (11) at the physical extremities $z=0$ and $z=d$. In terms of the variables, ϕ and s, these are given explicitly by

$$-\epsilon_{\rm I}\kappa_p \ln[\phi(0)/\xi] + \epsilon_{\rm II}\kappa \left.\frac{d\phi}{ds}\right|_0 \frac{1}{\phi(0)} = -\frac{q\beta\sigma_p}{\epsilon_0},$$

$$\epsilon_{\rm III}\kappa_n \ln[\phi(\kappa d)/\xi] + \epsilon_{\rm II}\kappa \left.\frac{d\phi}{ds}\right|_{\kappa d} \frac{1}{\phi(\kappa d)} = \epsilon_{\rm III}\kappa_n q\beta V_D + \frac{q\beta\sigma_n}{\epsilon_0}. \tag{28}$$

Hence, inserting Eq. (27) into this system we obtain

$$\epsilon_{\rm II}\kappa\frac{(1-\xi^2)}{\xi^{1/2}}\left.\frac{\mathrm{sc}}{\mathrm{dn}}\right|_{s_0/2\xi^{1/2}} + 2\epsilon_{\rm I}\kappa_p \ln\left(\xi\,\mathrm{cd}\Big|_{s_0/2\xi^{1/2}}\right) = -\frac{q\beta\sigma_p}{\epsilon_0},$$

$$\epsilon_{\rm II}\kappa\frac{(1-\xi^2)}{\xi^{1/2}}\left.\frac{\mathrm{sc}}{\mathrm{dn}}\right|_{(s_0-\kappa d)/2\xi^{1/2}} - 2\epsilon_{\rm I}\kappa_p \ln\left(\xi\,\mathrm{cd}\Big|_{(s_0-\kappa d)/2\xi^{1/2}}\right)$$

$$= -\epsilon_{\rm III}\kappa_n q\beta V_D - \frac{q\beta\sigma_n}{\epsilon_0}. \tag{29}$$

where dn and sc are two other elliptic functions [38–40]. As

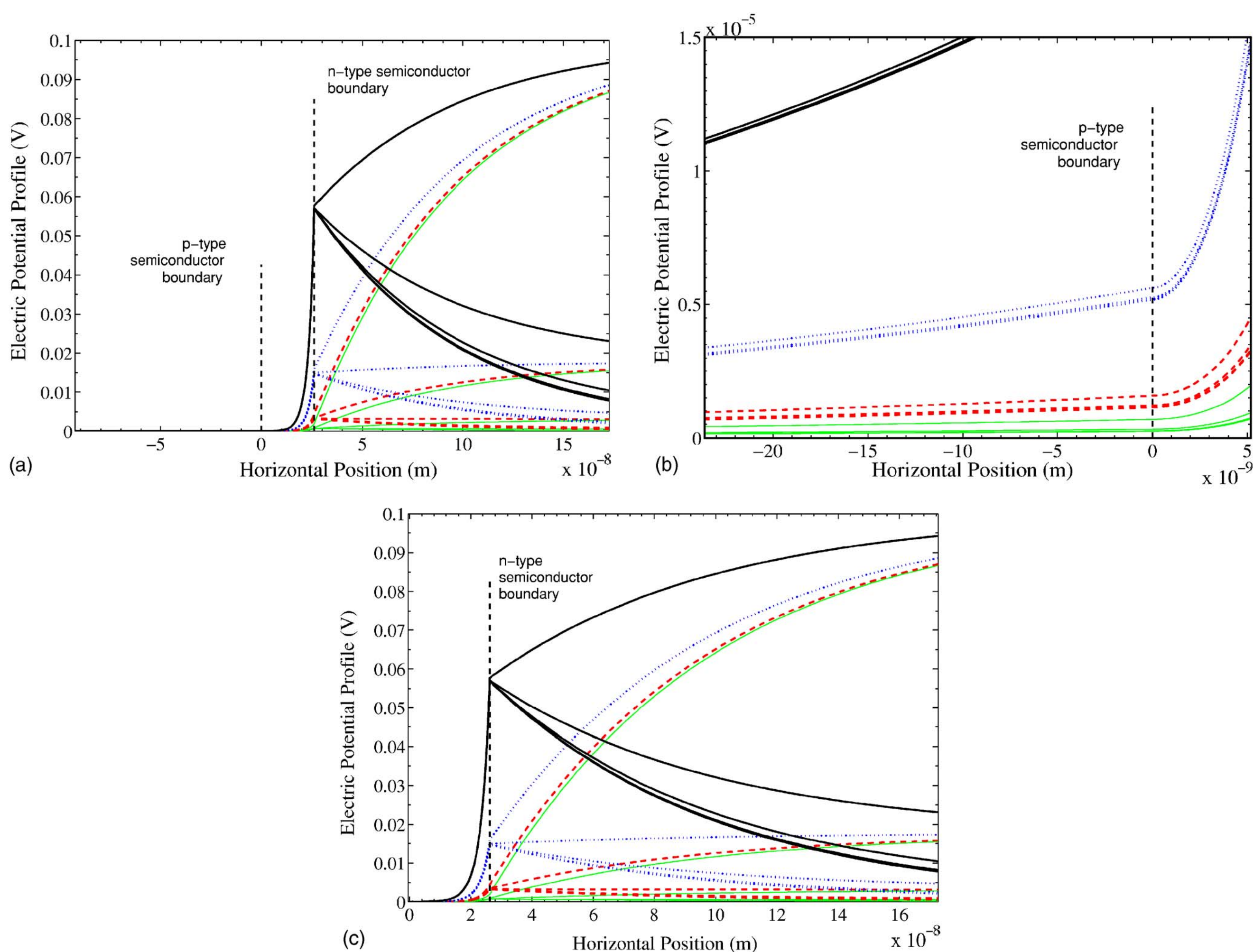

FIG. 2. (Color online) Electrostatic potential profile across the *pen*-heterojunction. (a) An overview across the entire heterojunction. (b) and (c) show detailed views in the p-type and n-type semiconductor regions, respectively. Here, $\sigma_p = 0.0$ C m^{-2} and $c_e = 10.0$ mM, while for each set (bottom to top of figure) $\sigma_n = 1.60$ (solid green lines), 7.44 (dashed red lines), 34.52 (dotted blue lines), 160.2 (solid black lines) $\times 10^{-4}$ C m^{-2} and for each σ_n set, the applied voltages from bottom to top are $V_D \in \{1.0, 5.62, 31.62, 177.83, 1000.0\} \times 10^{-4}$ V. The electrolyte thickness is $d = 26.25$ nm. Other system parameters are $\epsilon_{\rm I} = 10$, $\epsilon_{\rm II} = 78.5$, $\epsilon_{\rm III} = 25$ $T = 298$ K, $p_p = 10^{-6}$ M, $n_n = 10^{-5}$ M.

in the counterion only case, the roots of this system of transcendental equations must be solved numerically for the values of s_0 and ξ.

IV. NUMERICAL RESULTS AND DISCUSSION

For all the cases shown in this section we assume a symmetric univalent electrolyte in the intermediate region. Secondly, we point out that most surfaces when immersed in an electrolyte solution acquire a surface charge either by adsorption of ionic species or dissociation of outerlying surface groups. This contingency, which does not normally arise in standard *pin*-heterojunctions, is taken into account. Such mechanisms are over and above those that can lead to an effective surface charge at the free surface of a semiconductor due to surface bound electronic states with forbidden bandgap energies as was discussed earlier [36]. For generality we consider the influence of surface charges on both semiconductor interfaces. All results shown here agree with those found by numerically solving the nonlinear PB equation in the electrolyte region employing the linear approximations in the semiconductor media. A user-friendly, executable program, valid for arbitrary electrolyte, is available from the authors. No attempt has been made to solve the model involving fully nonlinear differential equations in all three regions. Nor have the approximations outlined in Secs. III A and III B been compared with full numerical solutions.

The full extent of parameter space representing this system has quite a few more dimensions than typically considered in the double layer literature and not possible to fully explore here. Fortunately, it is not necessary to completely cover the entire spectrum of values in order to get a qualitative feel for the system's dependence on these parameters. Potential profiles spanning the three regions of p-type semiconductor, electrolyte, and n-type semiconductor are shown in Figs. 2–7 and 14, for a range of electrolyte concentrations, n_e, surface charge on the n-type semiconductor surface σ_n and net difference potential V_D. In the outer media, depths of only two decay lengths κ_p and κ_n are explicitly represented. The results shown in these figures and the discussion below

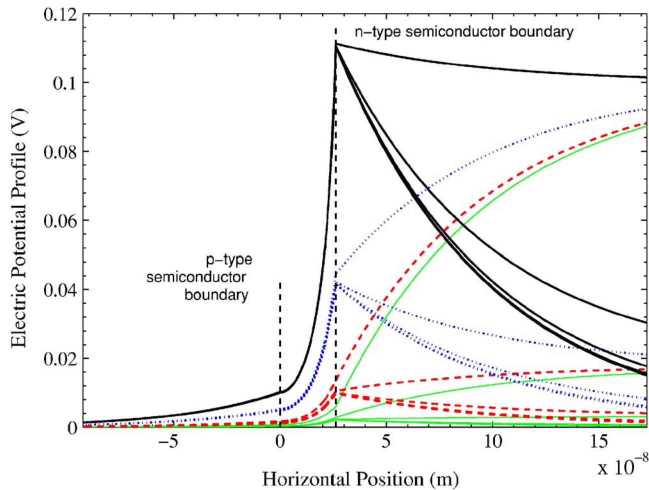

FIG. 3. (Color online) Electrostatic potential profile across the *pen*-heterojunction. Numerical details as in Fig. 2, except $c_e = 1.0$ mM and only the overview is shown.

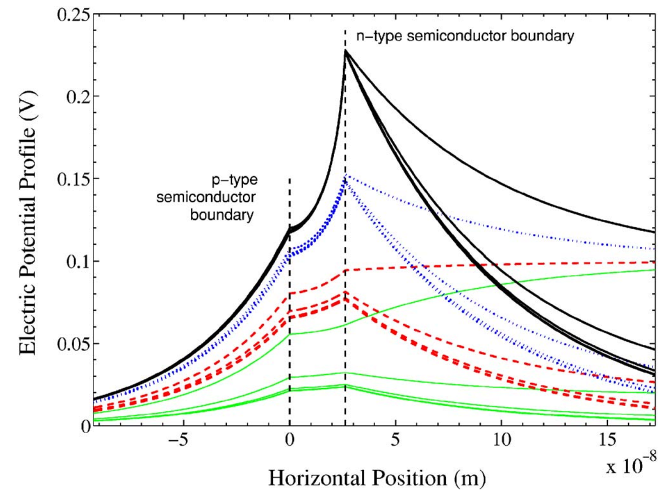

FIG. 5. (Color online) Electrostatic potential profile across the *pen*-heterojunction. Numerical details as in Fig. 2, except $c_e = 0.01$ mM and only the overview is shown.

indicate some of the general trends as electrolyte concentration, magnitude of surface charge σ_n and applied potential are increased. Generalizations to other cases not explicitly presented here can readily be made.

Figures 2–7 [specifically (a) in Fig. 2] give an overview of the dependence of the electric potential on σ_n and V_D for $\sigma_p = 0$ and for a single (arbitrary) electrolyte thickness of $d = 26.3$ nm. Irrespective of σ_n, the potential to the extreme right of the *n*-type semiconductor region tends to the stipulated value of V_D. The curvature of the profile here depends on the potential value on the interface $z = d$, which, for electrolyte concentrations of 10^{-2} and 10^{-3} M, is largely governed by the value of the surface charge on this interface. The dominant role played by σ_n over V_D extends into both the electrolyte region as well as into the *p*-type semiconductor. It is only for very low surface charges that the applied potential makes any quantitative impact on the potential values either at or to the left of the boundary at $z = d$. This is more apparent in Figs. 4 and 5. Furthermore, the sequence of Figs. 2–5 suggests that this domination decreases as the electrolyte concentration decreases. We then infer that the electrolyte screens the *p*-type semiconductor from the potential applied at the extreme right of the *n*-type semiconductor. Moreover, this screening is most effective when there is a substantial surface charge on (at least) the *p*-type semiconductor interface since this draws in more ions from the bulk. This behavior may have some practical importance for device design.

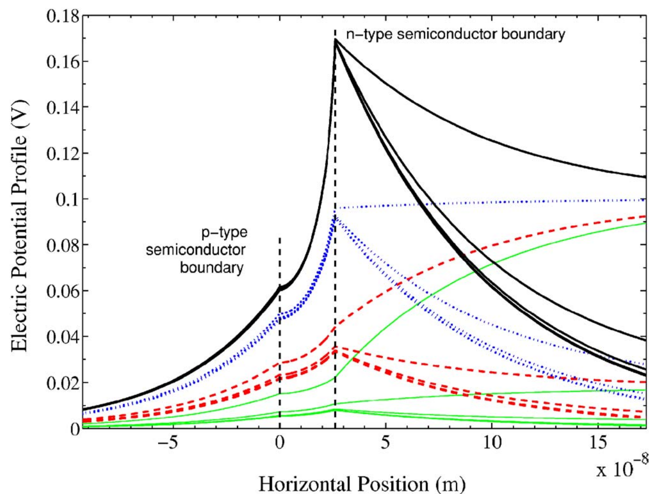

FIG. 4. (Color online) Electrostatic potential profile across the *pen*-heterojunction. Numerical details as in Fig. 2, except $c_e = 0.1$ mM and only the overview is shown.

Qualitatively different looking profiles appear when both surfaces possess a finite charge of opposite sign. In the case shown in Figs. 6 and 7 the *p*-type semiconductor possesses a

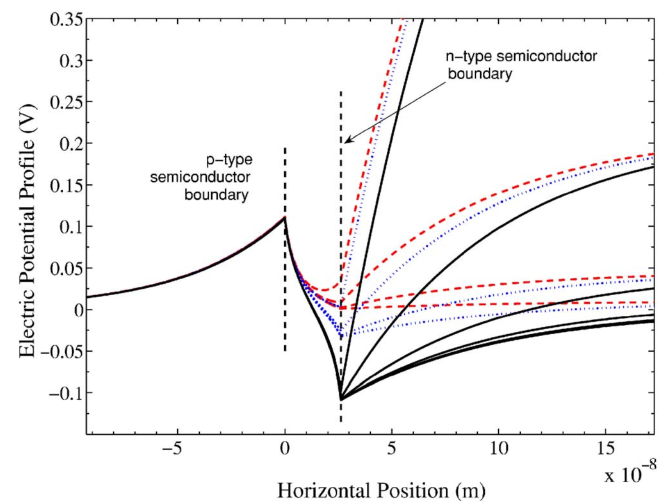

FIG. 6. (Color online) Electrostatic potential profile across the *pen*-heterojunction. Here, $\sigma_p = +1.6 \times 10^{-2}$ C m^{-2} and $c_e = 1.0$ mM. For each set (top to bottom of figure) surface charges on the *n*-type semiconductor are $\sigma_n = -1.60$ (solid green lines), -7.44 (dashed red lines), -34.52 (dotted blue lines), -160.2 (solid black lines) $\times 10^{-4}$ C m^{-2} and for each σ_n, the applied voltages from bottom to top are $V_D \in \{1.0, 4.64, 21.54, 100.0\} \times 10^{-2}$ V. Other system parameters are as in Fig. 2.

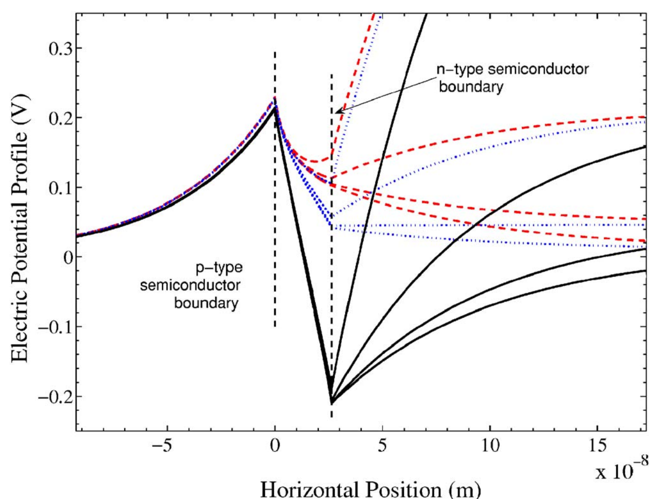

FIG. 7. (Color online) Electrostatic potential profile across the *pen*-heterojunction. Numerical details as in Fig. 6, except c_e =0.01 mM.

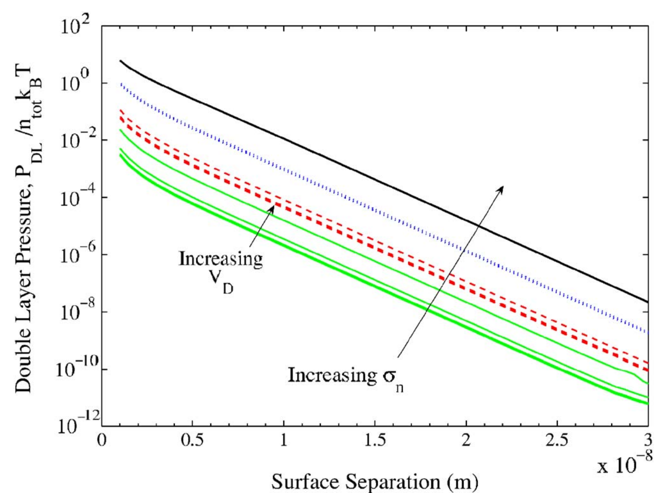

FIG. 8. (Color online) Double layer pressure as a function of thickness of electrolyte medium d. Numerical details as in Fig. 2.

(fixed) positive surface charge $\sigma_p=0.016\ \mathrm{cm}^{-2}$, while the n-type semiconductor carries a negative surface charge $\sigma_n<0$. For these cases, the contribution by the applied potential is of opposite sign to σ_n, so the effect of increasing V_D is to make the net effective surface charge on the n-type interface more positive. Once again, this effect is most clearly apparent when $|\sigma_n|$ is lowest. At the σ_n value of greatest magnitude, the potential again does not have any influence on the profile to the left of the right-hand boundary, even for the extreme value of $V_D=1$ V. More importantly, the potential profile in the p-type semiconductor is all but independent of either σ_n or V_D, especially at the higher electrolyte concentration, but also at the lower concentration. This we interpret as the influence of the surface charge σ_p on the interface at $z=0$; the electrolyte here serves only to influence the height of the potential at $z=0$, through screening. We thus expect that increasing the electrolyte concentration will (a) further decrease the potential heights at the interfaces and (b) further reduce the impact of the applied voltage on the potential profile within both the electrolyte and the p-type semiconductor regions. Again, this behavior might have consequences for the design of electrolyte-semiconductor devices.

It is well known [8,24,41] that the double layer stress P_{DL} between two plane parallel surfaces separated by an isotropic electrolyte medium of thickness, d, can be determined via the kinetic-Maxwell stress formula [24,42]

$$P_{\mathrm{DL}}(d)=k_BT\sum_{i=1}^{N}[n_i(z)-n_i^0]-\frac{1}{2}\epsilon_0\epsilon_{\mathrm{II}}\left(\frac{d\psi(z)}{dz}\right)^2, \quad (30)$$

evaluated at any position z in the interval $[0,d]$, the natural choices for z being, of course, $z=0$ and $z=d$. We have employed this expression to generate the interaction data shown in Figs. 8–13. We remark first that the theoretical arbitrariness of the z point is not always numerically upheld in practice. Specifically, in those cases where the potential and field values at the left-hand boundary are small, the formula becomes unreliable and generally does not agree with the force value found using the field and potential on the right-hand boundary, which seems reliable at least out to separations of about 10 Debye lengths. On the other hand, once the potential and field values become sufficiently large (e.g., when the separation has decreased enough for the interaction to be significant) the two evaluations give identical results. To ensure general reliability and accuracy, data from the right-hand interface was routinely used for all the results explicitly shown here.

Although the difference potential V_D is a constant potential condition acting over the whole system, it comes into play as a constant surface charge term in the boundary condition at the right-hand interface, Eqs. (22), (23), (28), and (29), reinforcing a positive intrinsic charge σ_n and countering a negative intrinsic charge. Consequently, under all σ_n and V_D conditions the two interfaces bounding the electrolyte are effectively constant charge surfaces. All possible cases should then be consistent with the findings of McCormack *et al.* [41]. It should, for example, be expected that the interac-

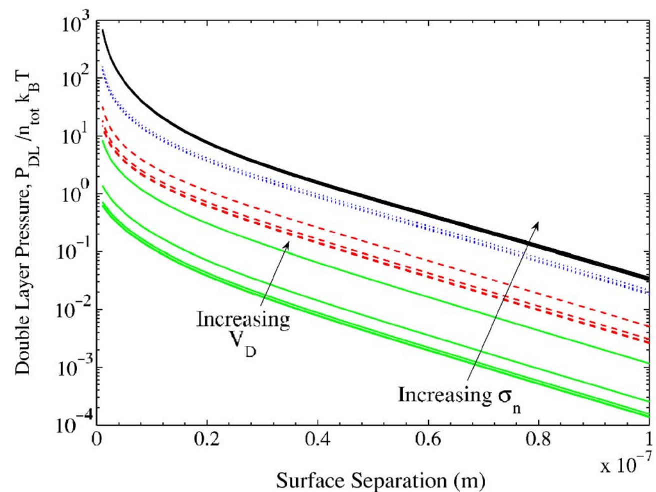

FIG. 9. (Color online) Double layer pressure as a function of thickness of electrolyte medium d. Numerical details as in Fig. 2, except $c_e=0.1$ mM.

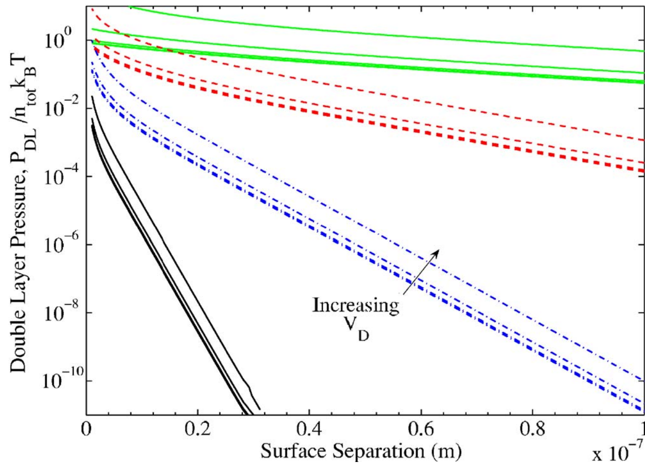

FIG. 10. (Color online) Double layer pressure as a function of thickness of electrolyte medium d. Force curve sets (top to bottom of figure) generated for $c_e=0.01$ (solid green lines), 0.1 (dashed red lines), 1.0 (dotted blue lines), 10.0 (solid black lines) mM. Within each set, the applied voltages from bottom to top are $V_D \in \{1.0, 5.62, 31.62, 177.83, 1000.0\} \times 10^{-4}$ V. Surface charge on the n-type semiconductor is $\sigma_n = 1.60 \times 10^{-4}$ C m^{-2}. Other system parameters are as in Fig. 2.

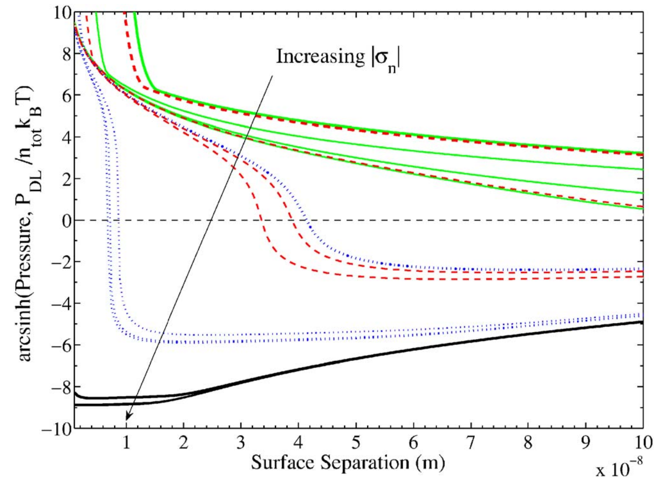

FIG. 12. (Color online) Double layer pressure as a function of thickness of electrolyte medium d. Numerical details as in Fig. 6, except $c_e=0.01$ mM.

tion will be repulsive under those conditions for which the constant charge surfaces are of like sign, including the case when one of the surfaces has zero charge, and be attractive at least at large separations, when the surfaces are of opposite sign. In the latter case the attraction could turn repulsive at short separations if the magnitude of the smaller charge is low enough. Consequently, we anticipate that in cases when they counteract, the force could possibly change from attractive to repulsive when the strength of V_D is large enough to compensate for σ_n.

When V_D reinforces σ_n, the repulsive pressure between the two semiconductor media show the same saturation phenomenon with surface charge as found with the potential profiles discussed above. For a given electrolyte concentration, it is only for the lower surface charges that the applied potential makes any quantitative difference to the interaction. Not surprisingly, increasing the potential increases the repulsion. For sufficiently large surface charges, however, increases in V_D do not affect the magnitude of the interaction. Fréchette and Vanderlick [28,29] reported a similar force saturation effect with applied potential for their mica-water-gold system. Although mica is an insulator and gold a conductor, the saturation phenomena in that system and in our model involving semiconductors might well have the same origin. For these strictly repulsive cases, the forces demonstrate the usual exponential decay with separation governed by the Debye length of the electrolyte medium κ. As found with the potential profiles, reducing the electrolyte screening allows for a greater variation in the pressure with V_D. This is again more pronounced at the lower surface charges. Whether these variations can be distinguished in actual force measurements is, however, to be seen.

Figures 11 and 12 show the double layer pressure for the case when the p-type semiconductor possesses a positive sur-

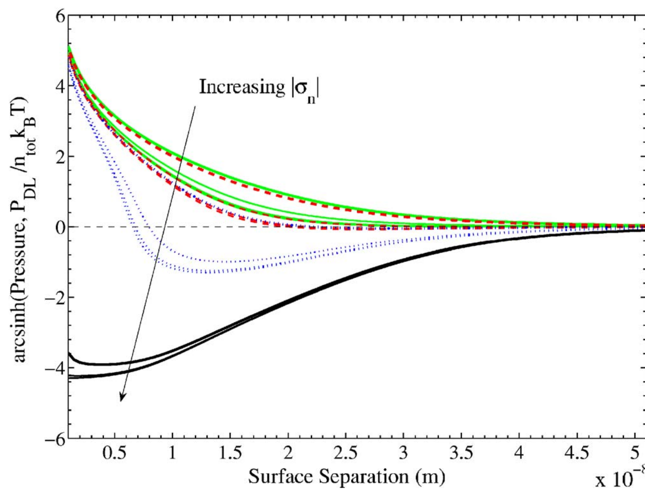

FIG. 11. (Color online) Double layer pressure as a function of thickness of electrolyte medium d. Numerical details as in Fig. 6.

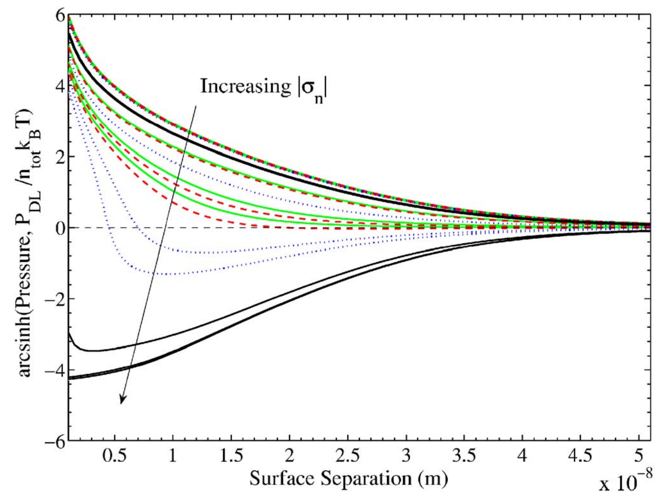

FIG. 13. (Color online) Double layer pressure as a function of thickness of electrolyte medium d. Numerical details as in Fig. 6, except $n_n=10^{-3}$ M.

face charge, while the n-type semiconductor possesses a negative surface charge, in competition with the positive applied potential. The results for these cases are shown on an arc-sinh scale in order to capture both attractive and repulsive interaction regions. Again, the qualitative behavior shown here is consistent with the analysis of McCormack *et al.* of constant charge surface interactions, for oppositely charged surfaces. At $c_e = 1$ mM, the forces for the two lowest (in magnitude) σ_n values exhibit a very weak, long-ranged attractive part when the positive applied potential is also low. But this attraction, at a given separation, quickly becomes a repulsion when V_D is increased, which results in a net effective positive surface charge on the n-type boundary. As σ_n becomes more negative, larger applied potentials are required to turn the interaction repulsive. The most negative value of σ_n corresponds, in the absence of V_D, to the fully antisymmetric surface charge system with the greatest magnitude attraction at all separations. In this case, not even a 1 V applied potential significantly affects the attraction, let alone converts it to a repulsion. At an electrolyte concentration two-orders of magnitude lower, the forces show analogous qualitative trends. We should point out that there is no physical attribute to the shoulder-like appearance of some of the curves, which is simply an artifact of the arc sinh scale (it would also appear with a sufficiently large linearly increasing force).

Finally, an increase in the electron concentration in the n-type semiconductor n_n achieved by increasing the doping concentration N_d [via Eq. (7)] results, somewhat counterintuitively, in more repulsive double layer forces as shown in Fig. 13. This can be understood by looking at the corresponding potential profiles shown in Fig. 14, which show that increasing n_n effectively brings the "point of application" of the external potential closer to the $z=d$ interface; the material becomes more conductorlike. The constraints on the potential and field at this interface give rise to more symmetric looking potential profiles within the electrolyte region. These in turn result in more repulsive forces.

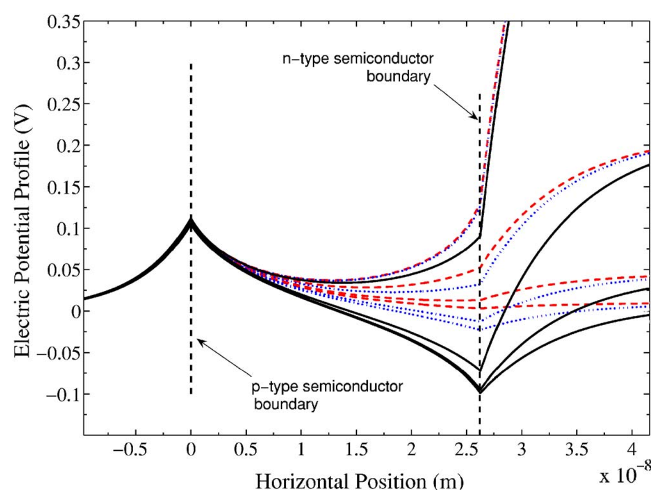

FIG. 14. (Color online) Electrostatic potential profile across the *pen*-heterojunction. Numerical details as in Fig. 6, except $n_n = 10^{-3}$ M.

V. CONCLUDING REMARKS

The extension of the ordinary double layer system to include effects of semiconductor properties of the materials bounding the electrolyte, as well as the effect of an externally applied potential, has been studied in this paper. Several features in both the electrostatic potential profiles in the three media and associated double layer forces have been found and discussed in terms of the functions' dependence on system parameters.

There are several avenues for further theoretical study that can be taken, the most important is the building-in of a self-consistent dependence of applied potential on surface charge properties (i.e., charge regulation). This should place the model on a more realistic standing. Another avenue of study involves replacing the solid semiconductors with porous organic polymer semiconductors, thus allowing for the migration of ions into the two outer media. Such a study is motivated by the current interest in organic polymer systems as cheap and environmentally friendly transistor devices [19–22]. Finally, the mean-field continuum model used here clearly ignores the finite sizes of both electrolyte ions and solvent molecules. However, with the application of strong electric fields as described here, discrete ion/solvent effects are likely to contribute significantly to the final forces. These, as well as possible dielectric saturation effects, should also be studied in a more refined model.

An experimental surface force study paralleling this theoretical modeling is highly desirable. The nature of the semiconductor media, however, may not be consistent with the current FECO method of determining the surface separation in the SFA. On the other hand, our results suggest that excessively thick semiconductor materials may not be necessary. In this case it might be possible to introduce partially reflective surfaces on the outer sides of the semiconductors in order to determine surface separations. While separation determination for this system might not be a problem with the AFM colloid probe technique, it may be necessary to provide an analogous sphere-flat model for a direct comparison between theory and experiment.

[1] E. J. W. Verwey and J. Th. G. Overbeek, *Theory of the Stability of Lyophobic Colloids* (Elsevier Press, Amsterdam, 1948).
[2] B. W. Ninham and V. A. Parsegian, J. Theor. Biol. **31**, 405 (1971).
[3] T. W. Healy, D. Y. C. Chan, and L. R. White, Pure Appl. Chem. **52**, 1207 (1980).
[4] D. Y. C. Chan and D. J. Mitchell, J. Colloid Interface Sci. **95**, 193 (1983).
[5] P. J. Richmond, J. Chem. Soc., Faraday Trans. 2 **70**, 1066 (1974); **71**, 1154 (1975).

[6] A. J. Kuin, Faraday Discuss. Chem. Soc. **90**, 235 (1990).
[7] S. J. Miklavic, D. Y. C. Chan, L. R. White, and T. W. Healy, J. Phys. Chem. **98**, 9022 (1994).
[8] S. J. Miklavcic, J. Chem. Phys. **103**, 4794 (1995).
[9] B. Duplantier, Physica A **168**, 179 (1990).
[10] A. Fogden, D. J. Mitchell, and B. W. Ninham, Langmuir **6**, 159 (1990).
[11] S. J. Miklavic, Philos. Trans. R. Soc. London, Ser. A **348**, 209 (1994).
[12] S. R. Dungan and T. A. Hatton, J. Colloid Interface Sci. **164**, 200 (1994).
[13] M. Kostoglou and J. Karabelas, J. Colloid Interface Sci. **171**, 187 (1995).
[14] J. E. Sader, J. S. Gunning, and D. Y. C. Chan, J. Colloid Interface Sci. **182**, 516 (1996).
[15] S. L. Carnie, D. Y. C. Chan, D. J. Mitchell, and B. W. Ninham, J. Chem. Phys. **74**, 1472 (1981).
[16] S. L. Carnie and G. Torrie, Adv. Chem. Phys. **56**, 141 (1984).
[17] L. Blum, Adv. Chem. Phys. **78**, 171 (1990).
[18] J. Lee and C. J. Kim, J. Microelectromech. Syst. **78**, 9 (2000).
[19] L. A. Majewski, R. Schroeder, and M. Grell, Adv. Mater. (Weinheim, Ger.) **17**, 192 (2005).
[20] M. J. Panzer, C. R. Newman, and C. D. Frisbie, Appl. Phys. Lett. **86**, 103503 (2005).
[21] F. Lin and M. C. Lonegran, Appl. Phys. Lett. **88**, 133507 (2006).
[22] M. J. Panzer and C. D. Frisbie, Appl. Phys. Lett. **88**, 203504 (2006); unpublished.
[23] J. N. Israelachvili and G. J. Adams, J. Chem. Soc., Faraday Trans. 1 **74**, 975 (1978).
[24] J. N. Israelachvili, *Intermolecular and Surface Forces*, 2nd ed. (Academic Press, New York, 1992).
[25] W. A. Ducker, T. J. Senden, and R. M. Pashley, Langmuir **8**, 1831 (1992).
[26] J. N. Connor and R. G. Horn, Langmuir **17**, 7194 (2001).
[27] D. A. Antelmi, J. N. Connor, and R. G. Horn, J. Phys. Chem. B **108**, 1030 (2004).
[28] J. Fréchette and T. K. Vanderlick, Langmuir **17**, 7620 (2001).
[29] J. Fréchette and T. K. Vanderlick, Langmuir **21**, 985 (2005).
[30] J. Fréchette and T. K. Vanderlick, J. Phys. Chem. B **109**, 4007 (2005).
[31] J. Wang, S. W. Feldberg, and A. J. Bard, J. Phys. Chem. B **106**, 10440 (2002).
[32] D. Barten, J. M. Kleijn, J. Duval, H. P. van Leeuwen, J. Lyklema, and M. A. C. Stuart, Langmuir **19**, 1133 (2003).
[33] R. P. Feynman, R. B. Leighton, and M. Sands, *Feynman Lectures in Physics* (Addison-Wesley, New York, 1965).
[34] S. M. Sze, *Physics of Semiconductor Devices*, 2nd ed. (Wiley, New York, 1981).
[35] H. T. Grahn, *Introduction to Semiconductor Physics* (World Scientific, Singapore, 1999).
[36] C. Kittel, *Introduction to Solid State Physics*, 7th ed. (Wiley, New York, 1996).
[37] S. J. Miklavic and B. W. Ninham, J. Theor. Biol. **137**, 71 (1989).
[38] E. T. Whittaker and G. N. Watson, *A Course in Modern Analysis*, 4th ed. (Cambridge University Press, Cambridge, 1927).
[39] P. M. Morse and H. Feschbach, *Methods of Theoretical Physics* (McGraw-Hill, New York, 1952), Vols. 1 and 2.
[40] M. Abramowitz and I. A. Stegun, *Handbook of Mathematical Functions* (Dover Publications, New York, 1970).
[41] D. McCormack, S. L. Carnie, and D. Y. C. Chan, J. Colloid Interface Sci. **169**, 177 (1995).
[42] J. D. Jackson, *Classical Electrodynamics*, 3rd ed. (Wiley, New York, 1999).